BJR https://doi.org/10.1259/bjr.20220339

Received: 24 March 2022 | Accepted: 22 February 2023 | Published online: 17 May 2023

Cite this article as:
Owens C, Hindocha S, Lee R, Millard T, Sharma B. The lung cancers: staging and response, CT, ^{18}F-FDG PET/CT, MRI, DWI: review and new perspectives. *Br J Radiol* (2023) 10.1259/bjr.20220339.

REVIEW ARTICLE

The lung cancers: staging and response, CT, ^{18}F-FDG PET/CT, MRI, DWI: review and new perspectives

[1]CARA OWENS, PhD FRCR MBBS BSc, [1,2]SUMEET HINDOCHA, PhD MRCP, MBBS, BSc, [1,3,4,5]RICHARD LEE, PhD, MRCP, MBBS, MA, [1]THOMAS MILLARD, PhD FRCR, MBBS, BSc and [1,3]BHUPINDER SHARMA, PhD FRCR, BM, BSc

[1]The Royal Marsden NHS Foundation Trust, Fulham Road, London, United Kingdom
[2]Artificial Intelligence for Healthcare Centre for Doctoral Training, Imperial College London, London, United Kingdom
[3]The Institute of Cancer Research, Sutton, United Kingdom
[4]National Heart and Lung Institute, Imperial College London, London, United Kingdom
[5]NIHR BRC at The Royal Marsden and the ICR, London, United Kingdom

Address correspondence to: Dr Cara Owens
E-mail: *c.owens22@imperial.ac.uk;cara.owens@nhs.net*

ABSTRACT

Lung cancer is the most commonly diagnosed cancer and the leading cause of cancer deaths in both sexes combined. Recent years have seen major advances in the diagnostic and treatment options for patients with non-small-cell lung cancer (NSCLC), including the routine use of 2-deoxy-2[^{18}F]-fluoro-D-glucose positron emission tomography/computed tomography (^{18}F-FDG PET/CT) in staging and response evaluation, minimally invasive endoscopic biopsy, targeted radiotherapy, minimally invasive surgery, and molecular and immunotherapies.

In this review, the central roles of CT and ^{18}F-FDG PET/CT in staging and response in both NSCLC and malignant pleural mesothelioma (MPM) are critically assessed. The Tumour Node Metastases (TNM-8) staging systems for NSCLC and MPM are presented with critical appraisal of the strengths and pitfalls of imaging. Overviews of the Response Evaluation Criteria in Solid Tumours (RECIST 1.1) for NSCLC and the modified RECIST criteria for MPM are provided, together with discussion of the benefits and limitations of these anatomical-based tools. Metabolic response assessment (not evaluated by RECIST 1.1) will be explored. We introduce the Positron Emission Tomography Response Criteria in Solid Tumours (PERCIST 1.0) to include its advantages and challenges. The limitations of both anatomical and metabolic assessment criteria when applied to NSCLC treated with immunotherapy and the important concept of pseudoprogression are addressed with reference to immune RECIST (iRECIST).

Separate consideration is given to the diagnosis and follow up of solitary pulmonary nodules with reference to the British Thoracic Society guidelines and Fleischner guidelines and use of the Brock (CT-based) and Herder (addition of ^{18}F-FDG PET/CT) models for assessing malignant potential. We discuss how these models inform decisions by the multidisciplinary team, including referral of suspicious nodules for non-surgical management in patients unsuitable for surgery. We briefly outline current lung screening systems being used in the UK, Europe and North America.

Emerging roles for MRI in lung cancer imaging are reviewed. The use of whole-body MRI in diagnosing and staging NSCLC is discussed with reference to the recent multicentre *Streamline L* trial. The potential use of diffusion-weighted MRI to distinguish tumour from radiotherapy-induced lung toxicity is discussed. We briefly summarise the new PET-CT radiotracers being developed to evaluate specific aspects of cancer biology, other than glucose uptake. Finally, we describe how CT, MRI and ^{18}F-FDG PET/CT are moving from primarily diagnostic tools for lung cancer towards having utility in prognostication and personalised medicine with the agency of artificial intelligence.

INTRODUCTION

Lung cancer is the most commonly diagnosed cancer and the leading cause of cancer deaths in both sexes combined.[1] The age-standardised 5-year net survival for lung cancer is in the range 10–20%.[2] Non-small cell lung cancer (NSCLC) is the most common type of lung cancer and includes adenocarcinoma, squamous cell carcinoma and large cell carcinoma.[3] Management of the lung cancer patient is influenced by the histopathological subtype, the molecular characteristics of the tumour and the stage of disease. Recent years have seen major advances in the diagnostic and treatment options for patients with NSCLC, including

the routine use of 2-deoxy-2-[^{18}F]fluoro-D-glucose (^{18}F-FDG) positron emission tomography/computed tomography (PET/CT) in staging and response evaluation,[4] minimally invasive endoscopic biopsy,[5] targeted radiotherapy,[6] minimally invasive surgery,[7] and molecular and immunotherapies.[8] It is incumbent on the radiologist to keep abreast of both therapeutic and imaging advances in order to optimise and accurately interpret imaging examinations in lung cancer patients.[9]

LUNG CANCER DIAGNOSIS AND STAGING

Whether identified through screening or a suspected cancer pathway, CT (low-dose CT (LDCT) in screening; typically i.v. contrast-enhanced CT in suspected cases), is the first modality for diagnosis and initial staging of lung cancer. Patients diagnosed with possible lung cancer are then offered ^{18}F-FDG PET/CT for staging completion. Currently, patients with stage II–IV disease are offered MRI brain for identification of cerebral metastases (UK National Institute for Health and Care Excellence (NICE) guidelines). The eighth edition of the Tumour, Node, Metastases (TNM) classification for NSCLC (TNM-8) (Table 1) is used to stage lung cancer. This is informed by sophisticated statistical analysis of an international database of over 100,000 patients.[11] TNM-8 can be applied to preoperative clinical staging, pathological staging, restaging post-therapy and staging of recurrence.[4]

The T element refers to the pre-operative primary tumour with size being important and progressive reduction in patient survival observed for each 1 cm cut point.[11,12] As Table 1 demonstrates, primary lung tumours (T) are categorised according to size from T1 to T4. The size of the primary is measured as the

Table 1. TNM-8 descriptors for NSCLC (Adapted from Carter *et al*, 2018 [10])

Category	Definition
T	
Tx	Primary tumour cannot be assessed, or tumour proven by non-radiological means (sputum or bronchial washings) and cannot be visualised with imaging (or bronchoscopy)
T0	No primary tumour
Tis	Carcinoma *in situ* (squamous or adenocarcinoma)
T1	Tumour ≤3 cm in greatest dimension
T1a T1b T1c	Tumour ≤1 cm
	Tumour >1 cm but ≤2 cm
	Tumour >2 cm but ≤3 cm
T2	Tumour >3 cm but ≤5 cm or tumour involving the main bronchus (regardless of the distance from the carina), the visceral pleura, with partial or complete lung atelectasis or pneumonitis
T2a T2b	Tumour >3 cm but ≤4 cm in greatest dimension
	Tumour >4 cm but ≤5 cm in greatest dimension
T3	Tumour >5 cm but ≤7 cm in greatest dimension or one that directly invades: parietal pleura, chest wall (including superior sulcus tumours), phrenic nerve, parietal pericardium, or separate tumour nodule or nodules in the same lobe
T4	Tumour measuring >7 cm in greatest dimension or which invades mediastinum, diaphragm, heart, great vessels, trachea, recurrent laryngeal nerve, oesophagus, vertebral body, carina; or separate tumour nodule(s) in a different lobe of ipsilateral lung
N	
N0	No regional lymph node metastases
N1	Ipsilateral peribronchial and/or ipsilateral hilar nodes and intrapulmonary nodes, including involvement by direct extension
N2	Ipsilateral mediastinal and/or subcarinal nodes
N3	Contralateral mediastinal, contralateral hilar, scalene, or supraclavicular nodes
M	
M0	No distant metastases
M1a	Separate tumour nodule(s) in the contralateral lung, malignant pleural effusion, pleural thickening/nodules or masses, malignant pericardial effusion/ pericardial thickening/nodules/masses
M1b	Single extrathoracic metastasis in a single organ (including non-regional lymph nodes)
M1c	Multiple extrathoracic metastases in a single organ or multiple organs

NSCLC, non-small cell lung cancer.

Figure 1. TNM staging in non-small cell lung cancer: Tumour (T) category. Tumour (T) classification is defined by the size of the primary lung tumour measured in the longest plane on CT on lung windows and by additional characteristics which affect the treatment options and prognosis. (**a**) Axial CT chest shows a 2.4 cm middle lobe tumour in a 65-year-old woman with emphysema, T1b disease. (**b**) Axial CT chest shows a 3.7 cm right upper lobe tumour in a 76-year-old woman, T2a disease. (**c**) Axial CT chest shows a 6.5 cm lingular tumour in a 70-year-old man with emphysema, T3 disease. (**d**) Coronal CT chest shows an 8 cm right upper lobe tumour in a 63-year-old woman which invades the superior vena cava, T4 disease. (**e**) Axial CT chest shows a 4.5 cm left upper lobe tumour with atelectasis, T2b disease. (**f**) Axial CT chest shows an 8 cm right lower lobe tumour with a further 2 cm tumour in separate lobe (right upper) of the ipsilateral lung, T4 disease. TNM, Tumour, Node, Metastases.

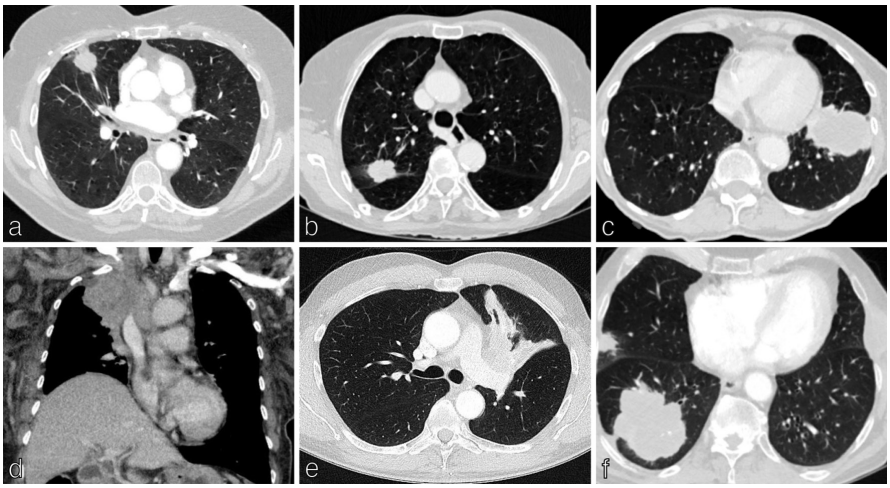

longest diameter in any plane on CT, on lung windows.[13] In part-solid tumours, the size of the solid component determines the T category (Figures 1a - 1c).[13] In addition to size criteria, T2–T4 descriptors assess further features of the primary malignancy which impact treatment options and survival. T2 descriptors include any size tumour which involves the main bronchus, invades the visceral pleura or is associated with atelectasis or pneumonitis (Figure 1e). T3 defines malignancies which invade parietal pleura, chest wall (including superior sulcus tumours), phrenic nerve, parietal pericardium or separate tumour nodule(s) in the same lobe. T4 descriptors include tumours greater than 7 cm and/or which invade mediastinum, diaphragm, heart, great vessels, trachea, recurrent laryngeal nerve, oesophagus, vertebral body, carina or separate tumour nodule(s) in different lobe of the same lung (Figures 1d and 1f).

Nodal (N) classification is defined by the involvement of intrathoracic lymph nodes and nodes are measured in shortest diameter. N1 refers to disease in ipsilateral peribronchial, hilar and intrapulmonary nodes (including from direct extension). N2 includes metastases in ipsilateral mediastinal and/or subcarinal nodes; patients can have single- or multistation N2 disease. N3 refers to disease in contralateral hilar, ipsi- or contralateral scalene, or supraclavicular lymph nodes. ^{18}F-FDG PET/CT plays a central role in mapping nodal disease in lung cancer and in identifying targets for histological sampling and radiotherapy planning (Figure 2a and 2b).[14] As described later in this review, potential nodal involvement usually requires histological confirmation. Metastatic disease burden is divided into M0, M1a (separate tumour nodule(s) in contralateral lung, malignant pleural effusion, pleural thickening/nodules/masses, malignant pericardial effusion, pericardial thickening/nodules/masses), M1b (single extrathoracic metastasis in a single organ) and M1c (multiple extrathoracic metastases in a single organ or multiple organs) (Figure 2).

SPECIAL CONSIDERATIONS: LUNG CANCER WITH MULTIPLE PRIMARY SITES OF INVOLVEMENT

In patients with more than one primary lung cancer, each malignancy should be staged separately, and this applies to both synchronous and metachronous lung cancers, regardless of location.[10] This can be challenging in clinical practice if the histology of the cancer is unknown and usual practice is to provide a range of stages *(e.g. T1a (multiple), or M1a)* and ensure that patients are not denied potentially effective treatment. Lung cancer can present as multiple ground-glass/part-solid nodules/masses on CT and these appearances are associated with lepidic adenocarcinoma, adenocarcinoma *in situ* or minimally invasive adenocarcinoma.[15] Classification is based on the lesion with the highest T-level (based on solid component) and the number of lesions (Figure 3b and c). A subset of lung cancers are defined as consolidative/pneumonic appearing on CT as consolidation and ground-glass opacification, often with air bronchograms (Figure 3a). Most pneumonic-type lung cancers are invasive mucinous adenocarcinomas, can be multicentric with metastases being rare at presentation.[15] In these cases, multiple sites of tumour involvement are designated T3 if they are confined to a single lobe and T4 if they affect different lobes of the same lung and M1a if both lungs are affected.

CT and ^{18}F-FDG PET/CT in staging NSCLC: strengths and pitfalls

In most cases, CT is the most suitable technique for defining the T category.[12] Assessment of nodal disease on CT considers

Figure 2. TNM staging in NSCLC-nodal (N) and metastatic (M) categories.Nodal (N) classification is defined by involvement of intrathoracic lymph nodes, measured in shortest diameter. ^{18}F-FDG PET/CT plays a central role in mapping nodal disease in lung cancer and in the identification of distant metastases. (**a**) N2 disease: fused, saggital ^{18}F-FDG PET/CT shows FDG-uptake in ipsilateral mediastinal lymph nodes in a 55-year-old man with a right upper lobe lung NSCLC (not imaged); nodal metastases were confirmed on EBUS-TBNA. (**b**) N3 disease: fused, coronal ^{18}F-FDG PET/CT shows FDG-uptake in bilateral mediastinal and right supraclavicular lymph nodes in a 50-year-old man with a 3 cm right lower lobe NSCLC (not imaged); nodal metastases were confirmed by ultrasound-guided biopsy of the right supraclavicular nodes. (**c**) M1C disease: axial CT of the abdomen shows bilateral adrenal metastases in a 65-year-old man with histologically confirmed NSCLC. (**d–f**) T4N2M1C disease in a 54-year-old patient with a left lung primary tumour shown on axial CT chest (**d**), ipsilateral mediastinal lymph nodes shown on coronal ^{18}F-FDG PET/CT (**e**), left pleural effusion and multiple liver metastases shown on coronal ^{18}F-FDG PET/CT (**e**) and coronal CT chest (**f**). EBUS-TBNA, endobronchial ultrasound-guided transbronchial needle aspiration; NSCLC, non-small cell lung cancer; TNM, Tumour, Node, Metastases.

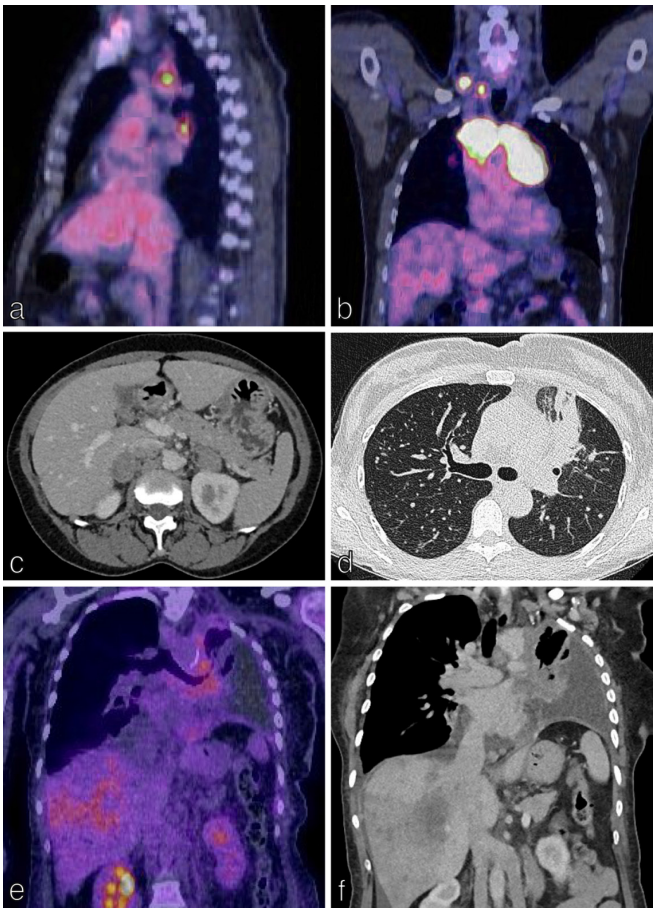

Figure 3. Lung cancer with multiple sites of involvement. (**a**) Axial CT chest of a 54-year-old ex-smoker presenting with bronchorrhea showing multiple areas of consolidation and ground-glass opacification; histologically confirmed as mucinous adenocarcinoma. (**b**) Axial CT chest of a 60-year-old female showing a 1.5 cm left upper lobe spiculate nodule histologically confirmed as NSCLC. Multiple ground-glass nodules bilaterally represent AIS/MIA. (**c**) Coronal CT chest of a 66-year-old female showing solid right upper lobe and left upper lobe tumours with peripheral ground-glass (largest 2.5 cm) plus multiple ground-glass opacities in the lungs; histologically proven as non-mucinous adenocarcinoma. These were staged as multiple synchronous primaries, T1C (multiple) disease. AIS, adenocarcinoma *in situ*; MIA, minimally invasive adenocarcinoma; NSCLC, non-small cell lung cancer.

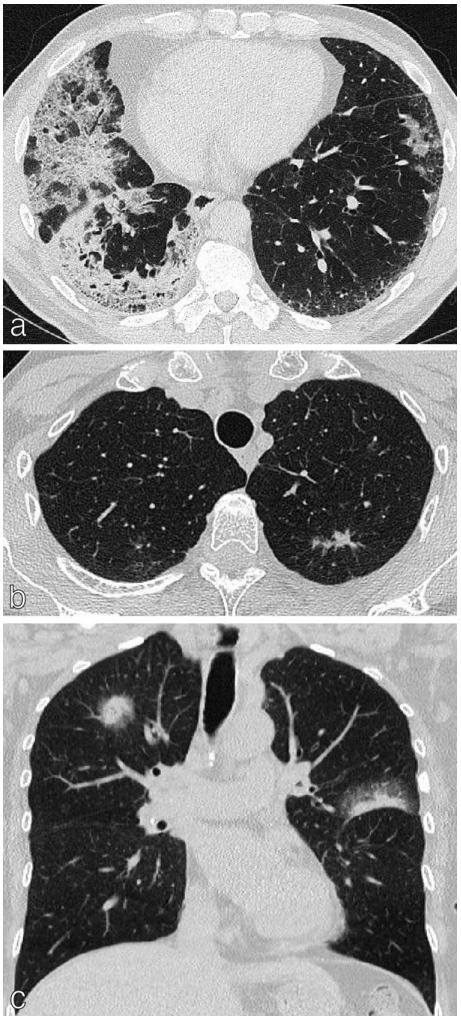

lymph nodes with short axis greater than 10 mm to be abnormal. However, studies show that this classical criterion has little diagnostic accuracy and that CT alone is suboptimal for nodal staging.[11,16] This is because factors other than size, *e.g.* density, enhancement, morphology and location are also important predictors of lymph node involvement.[17] Possible distant metastases (*e.g.* adrenal, liver, bone), identified on CT require further imaging for confirmation.

^{18}F-FDG PET/CT provides both anatomical and metabolic information with particular strengths in the assessment of lymph nodes and unanticipated Stage IV disease. Thus, ^{18}F-FDG PET/CT results can significantly impact on treatment

Figure 4. ^{18}F-FDG PET/CT is central to the accurate staging of NSCLC.^{18}F-FDG PET/CT is superior to CT in distinguishing tumour from rounded and post-obstructive atelectasis. (**a**) Axial CT chest of a 62-year-old man demonstrates a left upper lobe mass with atelectasis. (**b**) ^{18}F-FDG PET/CT in the same patient helps define the bronchogenic primary separate from the atelectasis enabling more accurate T-staging. (**c**) Axial CT chest of a 68-year-old man demonstrates a mass in the left lower lobe, estimated at 2.5 cm in diameter (T1C). Subtle pleural thickening in the left hemithorax is also present. (**d**) Axial ^{18}F-FDG PET/CT in the same patient demonstrates that the 2.5 cm mass is not PET-avid and is more consistent with rounded atelectasis. The bronchogenic primary measured only 9 mm. Additionally, there is FDG uptake in the left pleura. The ^{18}F-FDG PET/CT therefore changed the T staging to T1a and the M staging to M1a (avid pleural thickening; confirmed as NSCLC on pleural biopsy). (**e**) Sagittal ^{18}F-FDG PET/CT imaging for a 60-year-old patient with NSCLC demonstrates avid FDG uptake in the manubrium. (**d**) An undiagnosed pathological fracture (no history of trauma) was confirmed on the original staging CT, thereby upstaging the disease and changing management.

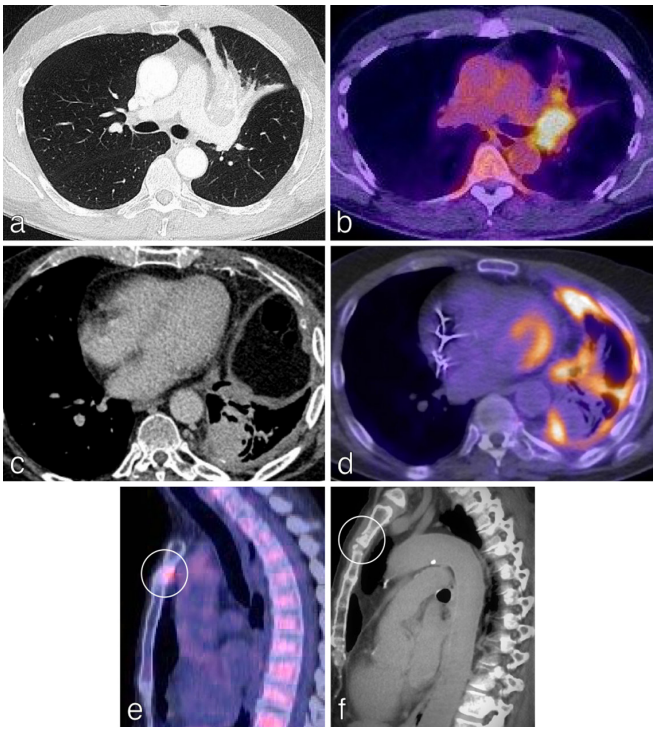

options and reduce the incidence of futile thoracotomies.[18–20] In a meta-analysis of 8699 patients, ^{18}F-FDG PET/CT had significantly higher sensitivity and specificity than CT alone in staging NSCLC.[21] Specifically, the pooled sensitivities and specificities of ^{18}F-FDG PET/CT were 0.72 and 0.91 for mediastinal nodal staging, 0.71 and 0.83 for intrathoracic staging, 0.75 and 0.95 for all extrathoracic metastases, 0.91 and 0.98 for bone metastases.[21] ^{18}F-FDG PET/CT plays less of a role in assigning the T-status, although it is superior to CT in enabling radiologists to distinguish tumour from rounded and post-obstructive atelectasis (Figure 4 a-d).[22] Uptake of FDG in lymph nodes (especially in patients with T1 disease) may help radiologists to identify smaller nodes which are involved. This improved sensitivity of ^{18}F-FDG PET/CT in identifying nodal disease is influenced by nodal dimension.[23] ^{18}F-FDG PET/CT is the chosen modality for assessing distant metastases (outside of the CNS). It has a higher sensitivity and specificity than bone scintigraphy for imaging bone metastases with a positive predictive value of 98% if there is PET and CT concordance (Figure 4e and f).[24]

There are important limitations to the use of ^{18}F-FDG PET/CT in staging NSCLC. In assessment of the T-status, false negatives can occur in nodules below 10 mm (T1a), low grade disease (Tis), minimally invasive adenocarcinoma (MIA), mucinous adenocarcinoma and well-differentiated carcinoid tumours (Figure 5a and b).[14] False positives can occur in infection, inflammation and granulomatous disease (Figure 5c and d). Nodal false positives can occur, *e.g.* in patients with TB or sarcoidosis,[21] whilst nodal false negatives can occur in small volume nodes (below the resolution of PET/CT) or those with low metabolic rate.[25] In terms of adrenal metastases, false positives (*e.g.* adrenal hyperplasia, functioning adenomas and tuberculosis) and false negatives (*e.g.* very small volume disease, haemorrhagic or necrotic metastases) must be considered. Importantly, it is not just the presence/absence of ^{18}F-FDG uptake in intrathoracic lymph nodes or adrenal glands that influences staging and treatment. The SUV_{max} is important and must be interpreted in the context of the avidity of the primary tumour and other imaging and clinical factors.[26] Intracranial metastases are better imaged using MRI due to the intrinsic high FDG uptake in the central nervous system (CNS). ^{18}F-FDG PET/CT findings suggestive for distant disease require either further radiological or histological confirmation and for mediastinal nodes, histological confirmation is needed as it affects management options (surgery/chemotherapy/radiotherapy).

Staging malignant pleural mesothelioma (MPM) (TNM-8)

MPM is a rare (incidence: approximately 30 cases/million in USA/UK), but very aggressive intrathoracic cancer with a very poor prognosis.[27,28] It is the most common primary malignancy of the pleura, associated with asbestos exposure in 80% of patients.[29] It consists of multiple nodules that may become confluent, spreading along pleural surfaces. There is often an associated pleural effusion (this may be the only finding on CT), thoracic volume loss and many patients have pleural plaques (Figure 6a–6f).[29] The T component of the TNM classification is challenging to apply in MPM because of its unconventional growth pattern.[30] The T-staging classification is shown in Table 2. Notably, tumour volume is not one of the main descriptors of disease burden even though it affects prognosis.[31] There are significant survival differences between T4 *vs* T3 disease and T3 *vs* T2 disease.[32] The N-component is an important prognostic indicator for survival in MPM as patients with nodal disease have significantly lower survival rates that those without.[33] N1 disease refers to ipsilateral bronchopulmonary, hilar or mediastinal nodes and N2 to contralateral intrathoracic and supraclavicular nodes. Distant metastases in MPM are designated M1 disease and is the only M status which determines Stage IV disease (Table 2; Figure 6).[34] Distant

Figure 5. False negatives and false positives on ^{18}F-FDG PET/CT. (**a**) Axial CT chest of a 72-year-old patient with confirmed adenocarcinoma *in situ* demonstrates a right upper lobe ground-glass opacity. (**b**) There was faint FDG uptake in the opacity (SUV_{max} less than the mediastinal blood pool); resulting in a low HERDER score. This is solely because of the ground-glass composition and emphasises the importance of interpreting FDG avidity carefully in each clinical context. (**c**) Axial ^{18}F-FDG PET/CT in a patient with a T1c primary NSCLC demonstrates FDG-avidity in bilateral hilar lymph nodes and a subcarinal node; suspected N3 disease. EBUS confirmed granulomatous cells and no malignancy, thereby a false-positive study. (**d**) Coronal ^{18}F-FDG PET/CT images of the thorax in an 88-year-old female presenting with trauma. The left upper lobe mass adjacent to the mediastinum is highly FDG-avid. CT-guided biopsy confirmed necrotising granulomatous disease with no malignant cells; thus a false positive. ^{18}F-FDG PET, 18-fludeoxyglucose positron emission tomography; EBUS, endobronchial ultrasound; NSCLC, non-small cell lung cancer; SUVmax, maximum standardized uptake value.

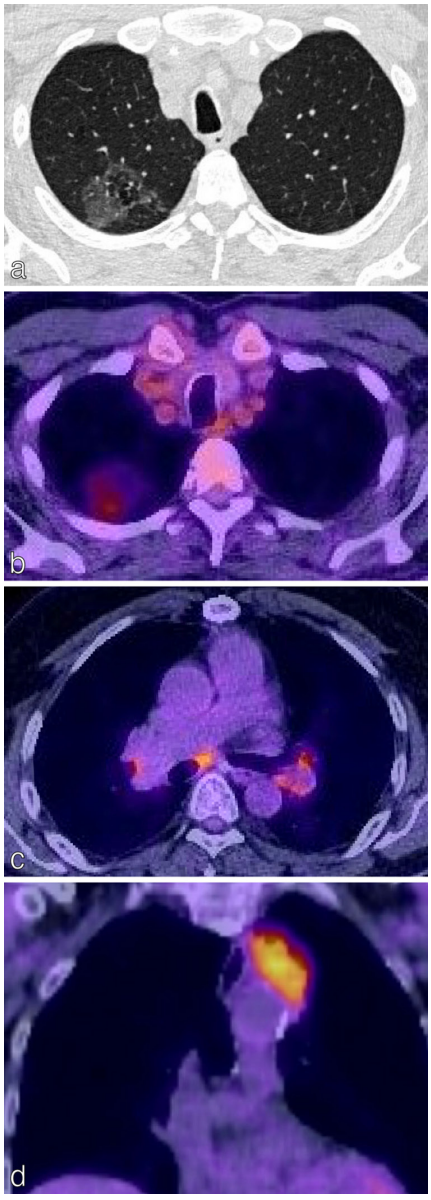

Figure 6. Staging malignant pleural mesothelioma (MPM). Axial CT images of the chest and upper abdomen on soft tissue windows in an 83y man presenting with chest pain shows irregular pleural thickening involving the right pleura (a) and including the mediastinal surface (b) with associated volume loss and a shallow right pleural effusion (c). A metastatic deposit is identified anterior to the stomach (c) making this stage IV disease; confirmed as epitheloid MPM on histology. Axial CT chest on soft tissue windows (d) and corresponding ^{18}F-FDG PET/CT (e, f) demonstrate a focus of irregular soft tissue in the pleura of the right upper lobe with invasion into the adjacent posterior chest wall, rib destruction plus a right pleural effusion, T4 tumour.

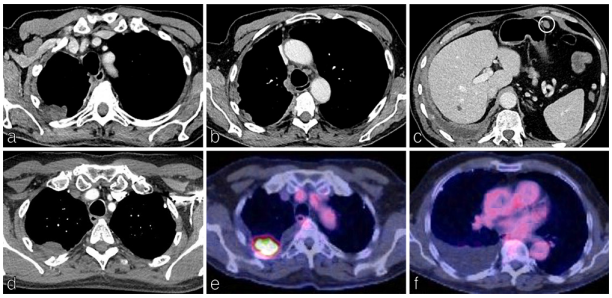

metastases are usually rare since patients often die from locally aggressive disease.[33]

CT has 68% sensitivity and 78% specificity for pleural malignancy but cannot reliably be used to differentiate MPM from pleural metastatic disease.[35] Although not routinely used, MRI, with its superior soft-tissue resolution over CT, improves identification of T3 disease and disease in the diaphragm, pericardium and chest wall.[36] In clinical practice, ^{18}F-FDG PET/CT is routinely used for staging and to guide surgical biopsy. Important limitations of ^{18}F-FDG PET/CT include its inability to differentiate between MPM and pleural metastases, and the fact that inflammatory disorders such as tuberculous pleurisy and prior pleurodesis can give false- positive results.[37] Importantly, pleurodesis-related ^{18}F-FDG PET-CT avidity can *"wax and wane"* for months to years following the procedure with consequent fluctuations in standard uptake value maximum (SUV_{max}) due to activated macrophages and granulation tissue. Regardless of the imaging modalities used to stage the disease, thorascopic biopsy is required for definitive diagnosis and staging of MPM.[33]

Solitary pulmonary nodules

Pulmonary nodules are focal densities ≤3 cm surrounded by aerated lung. The challenge is to discriminate between benign, inflammatory nodules (the vast majority; even in smokers) and those which represent pre-malignant, pre-invasive or early invasive adenocarcinoma.[38] Identification of early stage adenocarcinoma reduces mortality.[39] The 2015 guidelines from the British Thoracic Society (BTS) and the Fleischner Society guidelines (2017) [40] outline recommendations for the identification and follow-up of suspicious pulmonary nodules with areas of agreement and divergence between the two. In both guidelines, nodule follow-up is not recommended for nodules with clear features of benignity such as popcorn calcification (Figure 7a)

Table 2. Modified eighth TNM descriptors for staging malignant pleural mesothelioma. Adapted from Berzenji *et al*., 2018

Category	Definition
	T
Tx	Primary tumour not assessable
T0	No evidence of a primary tumour
T1	Tumour involving the ipsilateral parietal pleura (including mediastinal and diaphragmatic pleura) with or without involvement of the visceral pleura
T2	Tumour involving each of the ipsilateral pleural surfaces (parietal, mediastinal, diaphragmatic and visceral) with at least one of the following: • Confluent visceral pleural tumour—including the fissures • Involvement of the diaphragmatic muscle • Invasion of the lung parenchyma
T3	Tumour involving all of the ipsilateral pleural surfaces (parietal, mediastinal, diaphragmatic and visceral) with at least one of the following features: • Invasion of the endothoracic fascia • Extension into the mediastinal fat • Solitary, completely resectable focus invading soft tissues of the chest wall • Non-transmural involvement of the pericardium
T4	Tumour involving all of the ipsilateral pleural surfaces with at least one of the following features: • Diffuse or multifocal soft tissue invasion of the chest wall • Any rib involvement • Invasion of the peritoneum through the diaphragm • Invasion of any mediastinal organ • Direct extension to the contralateral pleura • Invasion of the spine or brachial plexus • Transmural invasion of the pericardium (with or without a pericardial effusion) • Myocardium invasion
	N
Nx	Regional lymph nodes not assessable
N0	No regional lymph nodes metastases
N1	Metastases in ipsilateral bronchopulmonary, hilar or mediastinal lymph nodes (including the internal mammary, peridiaphragmatic, pericardial fat pad or intercostal lymph nodes)
N2	Metastases in the contralateral bronchopulmonary, hilar or mediastinal lymph nodes or ipsilateral or contralateral supraclavicular lymph nodes
	M
Mx	Presence of distant metastases not assessable
M0	No evidence of distant metastases
M1	Evidence of distant metastases

or for nodules with "typical" perifissural or subpleural location with triangular or lentiform shape (often intrapulmonary lymph nodes) (Figure 7b) or for nodules <5 mm (<80 mm^3) (BTS) or <6 mm (Fleischner). In both guidelines, recommendations for nodules not considered definitely benign are informed by the composition of the nodule (solid, part-solid, ground-glass), followed by nodule size and assessment of risk of malignancy (nodule characteristics and patient risk factors).[41] The guidelines differ in a number of respects, such as the scope and target populations, definition of substantial growth, follow-up intervals and components of the risk assessment.[41]

The BTS guidelines are applied to nodules detected both incidentally and in screening. In BTS, CT surveillance is offered to patients with nodules ≥5 to<8 mm (≥80 to <300 mm^3). Automated or semi-automated volumetry is preferred over diameter measurements as it is more reproducible. In nodules ≥300 mm^3 or ≥8 mm, the pre-test probability of malignancy is assessed using the Brock Risk Prediction Tool which is derived from a study of two cohorts of current or former smokers undergoing LDCT.[42] Factors including family history of lung cancer, emphysema, larger nodule size, nodule location in the upper lobe, part-solid type and spiculation are considered malignant features.[42] Nodules which are risk stratified as having a <10% risk of malignancy using Brock are followed up on imaging (Figure 7c–e). Nodules with a ≥10% risk of malignancy are referred for ^{18}F-FDG PET/CT (provided they are larger than local PET-CT threshold) with post-test probability of malignancy assessed by the Herder model (Figure 7f–h).

Figure 7. Identification and follow up of pulmonary nodules. In both the BTS and Fleischner guidelines, nodules with clear features of benignity are not followed up. (a) Axial chest CT of a 66y smoker shows a left lower lobe nodule with calcification and central fat attenuation typical for a hamartoma; no follow up. (b) Coronal chest CT in a 60y smoker shows a lentiform/triangular shaped nodule associated with the horizontal fissure, typical for intrapulmonary lymph node; no follow up. The risk of malignancy in pulmonary nodules can be calculated using the Brock risk prediction tool. Nodules with < 10 % risk malignancy which are 80 mm^3 (6mm) are followed up at three months and one year from baseline. (c-e) Axial CT chest imaging of an incidentally detected 9mm right upper lobe solid pulmonary nodule at baseline (c), 3 months (d) and one year (e) demonstrates stability based on the 2D non-automated diameter; plan for follow up 2 years from baseline as assessed under the BTS guidelines. Nodules showing clear growth (25 % volume increase/volume doubling time (VDT) of < 400 days) undergo further diagnostic work-up with ^{18}F-FDG PET/CT /biopsy. (f-h) A 17mm left upper lobe nodule assessed at baseline (f) and at year 1 (g). Clear growth was demonstrated with more than 25 % increase in volume. The SUVmax on ^{18}F-FDG PET/CT was 2.83 (moderate) (h) with a Herder score of 89.1 % and subsequent plan for image-guided biopsy and MDT discussion regarding treatment options.

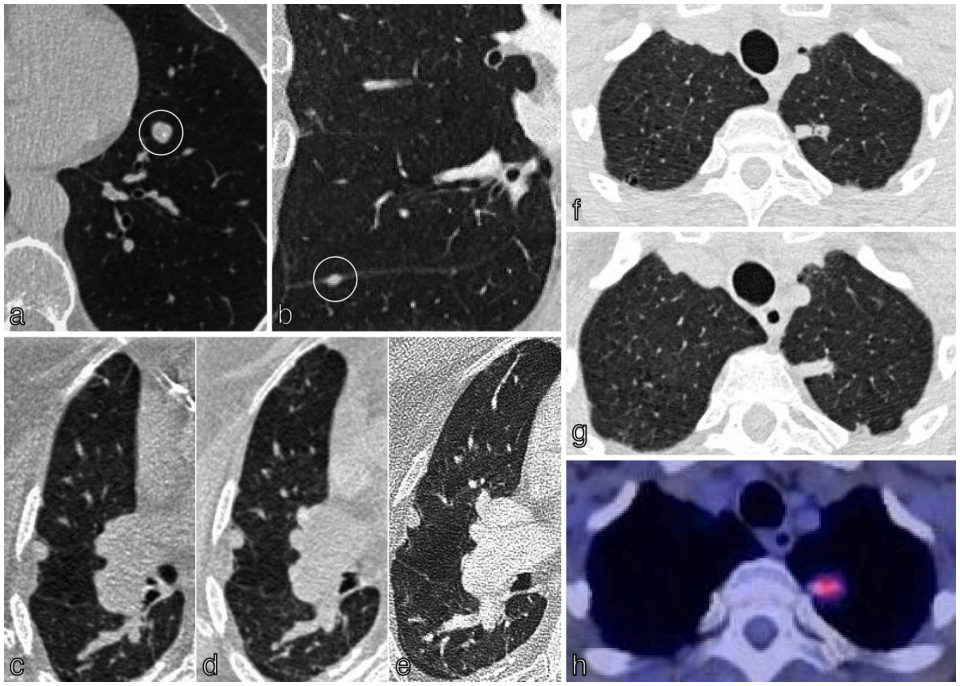

In the Herder model, an ordinal scale is used to define tracer uptake as absent (indiscernible from background lung tissue), faint (less than or equal to mediastinal blood pool), moderate (greater than mediastinal blood pool), or intense (markedly greater than mediastinal blood pool).[43] Although the Herder score was based on raw PET data, rather than the corrected data (as used in MDT discussions), it has been validated in a retrospective study.[44] Following Herder analysis, patients with a malignancy risk of >10–70% are offered image-guided biopsy, excision biopsy or CT surveillance. Patients with risk >70% are offered surgical resection (ideally by video-assisted thoracoscopic surgery), or non-surgical treatment, often with (although sometimes without) image-guided biopsy. The decision to refer patients with >70% risk of malignancy for non-surgical management (*e.g.* stereotactic ablative body radiotherapy (SABR), radiofrequency/microwave ablation, conventional radical radiotherapy) without histopathological confirmation, is a multidisciplinary one. The incorporation of clinically diagnosed lung cancer into the BTS guidelines reflects the findings of retrospective cohort studies showing similar outcomes between pathologically proven and clinically diagnosed early stage lung cancers in certain patient groups.[45–47] SABR, in particular, represents a significant advance in modern radiotherapy and provides targeted high doses in few fractions resulting in excellent local control and relatively minimal toxicity in standard-risk patients.[45,48]

For those nodules under CT surveillance, the BTS guidelines define significant growth as a ≥25% vol increase. Further diagnostic work-up should be offered for nodules showing clear growth or a volume-doubling time (VDT) of <400 days. Patients with stable solid nodules 1 year after baseline (based on VDT) or 2 years (based on two-dimensional measurements) can be discharged. Part-solid and pure ground-glass nodules are followed-up differently, reflecting their generally slower growth, but paradoxically higher malignant potential.

Lung screening

Targeted lung screening reduces disease-specific mortality and is now recommended by both the UK National Screening Committee (UKNSC) and the US Preventive Services Task Force (USPSTF).[49] In both screening programmes, current and former smokers aged 55–74 years (UKNSC) and 50–80 years (USPSTF) are invited for screening, (biennially in the UK; annually in North America), with LDCT. Reporting of screen-detected lung

nodules in the UK and Europe is based on the BTS guidelines.[50] The European position statement on lung cancer screening (2017) [50] recommends the use of volumetry and volumed-doubling time in risk assessment. In North America, the Lung CT Screening Reporting and Data System (Lung-RADS) from the American College of Radiology (ACR) provides a standard method of reporting and managing screening-detected lung nodules.[51] It can reduce the false-positive rate without increasing the rate of false negatives and is now routinely used in this screening population.[52,53] In this tool, the diameter (rather than the volume), of the dominant solid, part-solid or ground-glass nodule is used to risk-stratify nodules into five categories: 1, negative; 2, benign; 3, probably benign; 4A, suspicious; 4B, very suspicious. Suggested clinical management is annual repeat LDCT for categories 1 and 2, 6 month follow-up LDCT for category 3 nodules; either 3 month repeat LDCT or ^{18}F-FDG PET/CT for 4A and chest CT, ^{18}F-FDG PET-CT and/or biopsy for category 4B.[54,55] Notably, in both the BTS and the Lung-RADS systems, the follow-up and management of ground-glass nodules remains challenging, especially when found in younger patients.[55] Special consideration must be given to "incident" nodules detected in lung screening. These are nodules which are were not present at baseline and are therefore potentially fast-growing and have a high cancer risk of 2–8%.[50] In Europe, proposed follow-up protocols for these nodules are therefore different from baseline nodules.[50] It is likely that nodule management protocols will continue to evolve as lung screening programmes are implemented more widely.

RESPONSE TO TREATMENT

RECIST 1.1

Accurate and timely assessment of response to treatment (tumour shrinkage; time to progression) is vital in order to optimise patient outcomes.[56] RECIST 1.1 (Response Evaluation Criteria in Solid Tumours) uses changes in tumour burden on CT/MRI to assess response to treatment (Figure 8). A maximum of five lesions are monitored for change in size (measured in one dimension; must be >10 mm on CT to be measurable) and/or two lesions per organ.[57] Pathological lymph nodes (nodes with a dimension 15 mm (short axis) and above) are considered measurable and are target lesions. Nodes that shrink to <10 mm short axis are considered normal. Response to treatment is described as: (i) complete response (CR, disappearance of all target lesions), (ii) partial response (PR, ≥30% decrease in tumour size from baseline), (iii) progressive disease (PD, ≥20% increase in tumour size) and (iv) stable disease (SD) (Figure 8).[58] Important caveats to diagnosing recurrence on CT alone include the difficulty in distinguishing between radiation-induced lung toxicity (RILT) and tumour-atelectasis complex formation; this is where other modalities can add benefit.[59]

Modified RECIST—MPM

The modified RECIST criteria were developed in 2004 to enable response evaluation in MPM, given its unique growth pattern.[60] In this system, tumour thickness perpendicular to the chest wall or mediastinum is measured in two positions at three separate levels on axial CT and the sum of these six measurements defines a pleural unidimensional measurement.[60] Treatment response is then assessed by measuring the same areas of pleura.

Figure 8. RECIST 1.1 in NSCLC. RECIST 1.1 uses changes in tumour burden on CT/MRI to assess response to treatment. Axial CT chest in a 62y patient with T1cN3M1c (brain, adrenal glands) NSCLC at baseline (a, c) and follow-up (b, d) demonstrates partial response (≥30 % decrease in tumour size from baseline) in a middle lobe primary tumour and subcarinal lymph nodes (white arrows). Treatment-related pneumonitis is evident on the follow-up study (black arrow; b). Contrast enhanced MRI brain in the same patient at baseline (e, g) and follow up (f, h) demonstrates complete response to treatment with disappearance of all target brain metastases.

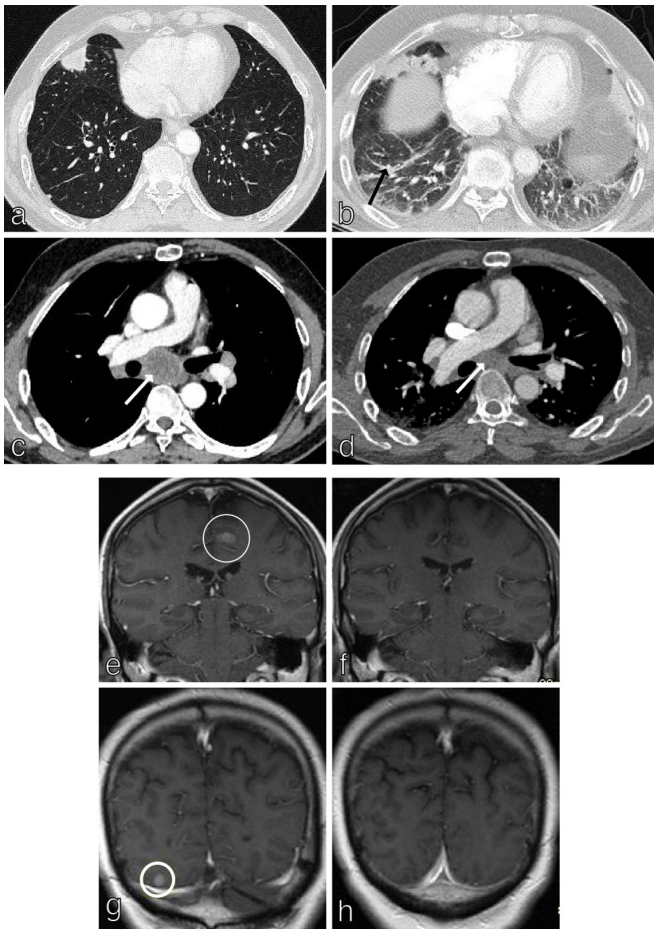

Measurable lesions such as nodes and subcutaneous nodules are assessed as per RECIST. CT remains the main modality to assess MPM but similarly to NSCLC, functional imaging techniques (PET, MRI-DWI, DCE-MRI) play a complementary role. There is great potential for the use of automated measurement of MPM and deep learning in order to address issues such as inter- and intraobserver variability and difficulties in distinguishing between pleural disease and pleural effusion.[61]

ASSESSING RESPONSE: BEYOND RECIST 1.1

Functional and metabolic imaging

Although RECIST 1.1 is validated in prospective studies and is used widely for response assessment, there are important limitations to assessing response based solely on size in lung cancer. Accurate and consistent measurement can be difficult in measuring ground-glass nodules, semi-solid nodules or

Table 3. Optimal time intervals proposed for response assessment using ^{18}F-FDG PET/CT Adapted from Kandathil *et al*., 2019)

Therapeutic modality	Time interval
Chemotherapy	10 days
Surgery	6 weeks
Radiofrequency ablation	6–8 weeks
Immunotherapy	8–9 weeks
Radiotherapy	3 months

^{18}F-FDG PET, 18-fludeoxyglucose positron emission tomography.

invasive lepidic carcinoma.[58,62] Markers of disease response such as density, functional and metabolic changes are not evaluated by RECIST 1.1. Metabolic responses and necrosis often precede size changes, especially in the context of cytostatic agents and immunotherapy. Techniques such as dual-energy CT, ^{18}F-FDG PET/CT, MRI and diffusion-weighted imaging (DWI)-MRI are increasingly used to provide functional and metabolic information in both assessment and prediction of response to treatment.[58] Analysis of tumour textural heterogeneity (marker for vascularity), tumour density (marker for necrosis) analysed on CT, CT perfusion studies in anti-angiogenic chemotherapy agents and dual-energy CT have been evaluated in response assessment in a bid to move beyond size alone.[63–66] These techniques provide useful predictive information but are not currently in widespread clinical use and in many cases require high quality and reproducible protocols for analysis.

^{18}F-FDG PET/CT has high diagnostic accuracy in detecting tumour recurrence with the added value of detecting metastases post-treatment.[67] However, timing of follow-up is vital as false positives can occur in post-treatment inflammation and radiation-induced lung toxicity (RILT) (Table 3).[56,67] In 2009, PET response criteria (PERCIST 1.0) were developed for systematic and structured assessment of response for use in clinical trials and potentially in the clinic.[68] In PERCIST 1.0, the peak SUV corrected for lean body mass (SUL_{peak}) is measured in the single "hottest" tumour. To be measurable at baseline this must be ≥ 1.5 times the mean SUL plus two times its standard deviation. The mean SUL is usually measured in a 3 cm diameter spherical volume of interest (VOI) in the right side of the liver.[69] Briefly, response is assessed as complete (^{18}F-FDG uptake less than mean SUL of liver), partial (decrease of ≥30% and of at least 0.8 SUL units in the most intense lesion (not necessarily the same lesion)), stable (increase or decrease of SUL_{peak}<30%) or progressive (increase of ≥30% and an increase of at least 0.8 SUL units in a target lesion or development of a new lesion).[69] Challenges remain in the interpretation of response using PERCIST 1.0, including assessing the behaviour of non-target lesions, a lack of definition for unequivocal progression, how to categorise new lesions as well as multiple technical factors such as accurately defining SUL_{peak}, accurately registering serial images from the same patient, selecting the mean SUL in the liver and comprehensively monitoring all factors affecting SUV between studies.[69,70] Automated systems to assess early response may improve on these constraints.[70] PERCIST 1.0 offers great potential; not currently realised at present.

Figure 9. Response to immunotherapy: pseudoprogression. (a-d) Axial CT and corresponding axial ^{18}F-FDG PET/CT images from a 67y man with left lower lobe T2aN2M0 NSCLC commenced on immunotherapy (Durvalumab). CT images show an increase in the size of the lung primary between baseline (a) and follow-up (b) suggesting disease progression. However, the corresponding ^{18}F-FDG PET/CT images (c) and (d) demonstrate partial metabolic response in the tumour. MDT decision was therefore for the patient to remain on current treatment regimen with close surveillance imaging.

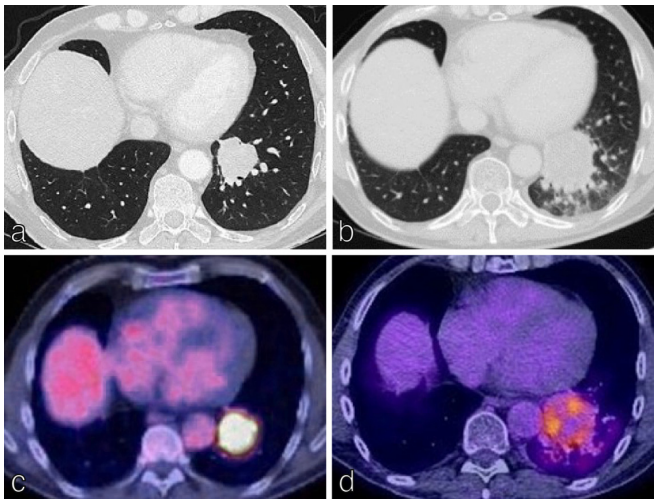

Response to immunotherapy

Tumours treated with immunotherapy (particularly immune checkpoint inhibitors), demonstrate unique response patterns which are not always assessable using classic RECIST 1.1. For example, an increase in tumour size after starting immunotherapy does not always represent progression but may be a result of T-cell infiltration and thus represent response.[71] Incidences of this "pseudoprogression" in patients receiving PD-1/PDL1 inhibitors in Phase II/III clinical trials can reach 10% (Figure 9).[72] Immune-specific response criteria including iRECIST (immunotherapy RECIST) that allow continued treatment beyond radiological progression have been developed for use in clinical trials.[72] The key change in iRECIST (compared to RECIST1.1) is the concept of resetting the bar if RECIST progression is followed at the next assessment by tumour shrinkage.[73] In iRECIST, response is designated as immune complete response (iCR), immune stable disease (iSD), immune partial response (iPR) and immune unconfirmed progressive disease (iUPD) or immune confirmed progressive disease (iCPD).[73] Definitions of CR, SD, PR and PD are unchanged from RECIST1.1. iUPD can be assigned multiple times provided that iCPD is not confirmed at the next assessment. Progression is confirmed in a target lesion if the next assessment after iUPD (4–8 weeks later) confirms a further increase in the sum of measures of target disease from iUPD, with at least 5 mm increase.[73] This means that patients who are designated as iUPD and not iCPD on follow-up studies can remain on therapy. However, these are not considered superior to RECIST 1.1 given the relatively low incidences of pseudoprogression and the added

Figure 10. AI: The radiomics workflow. Patients undergo medical imaging, *e.g.* CT, MRI or PET-CT. Regions of interest (ROI) *e.g.* a tumour are segmented either in 2D or 3D. Radiomic features are extracted from the ROI. Machine learning is applied to radiomic features to predict a given outcome *e.g.* benign vs malignant lung nodule. Machine learning models can be developed for disease classification, patient clustering, or risk stratification. Figure adapted with permission from: van Timmerman J *et al*. DOI: https://doi.org/10.1186/s13244-020-00887-2.

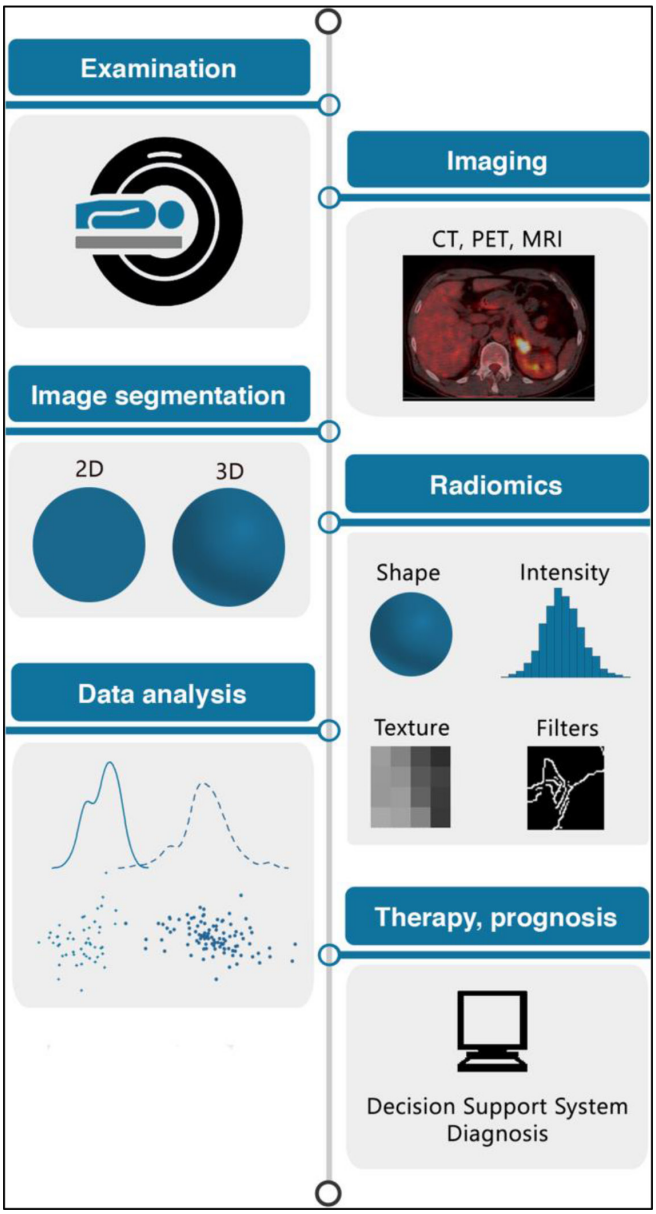

problem of hyperprogression that has been observed in 9–29% of patients treated with immunotherapy.[72,74,75]

FUTURE HORIZONS

As outlined earlier, the current diagnostic pathway for patients with newly diagnosed NSCLC involves a combination of CT, MRI and ^{18}F-FDG PET/CT. In this section, we review some of the new and emerging techniques which offer potential for improved accuracy of staging and response evaluation of NSCLC.

Whole-body MRI (WB-MRI)

A multicentre, prospective study in England (Streamline L trial) compared the diagnostic accuracy and efficiency of WB-MRI with standard staging pathways for metastatic disease in new NSCLC patients (destined for curative treatment). WB-MRI pathways had similar accuracy to standard pathways for T-staging but reduced sensitivities for nodal staging.[76] Diagnostic accuracy was similar to standard pathways for identifying metastatic disease but WB-MRI had improved performance in terms of time and cost efficiencies. Although generally underappreciated, reducing time to treatment is associated with improved survival and reduced patient anxiety.[77]

Diffusion-weighted magnetic resonance imaging (DW MRI)

When tumours respond to treatment we expect reduction in their cellularity. This can be measured as an increase in apparent diffusion coefficient (ADC) on DWI MRI.[78] A number of small studies indicate that ADC may be an independent marker of response of NSCLC to radiochemotherapy with potential to assess for early response, before reduction in tumour size.[78] As mentioned earlier, conventional CT or ^{18}F-FDG PET-CT imaging follow-up of NSCLC patients treated with radiotherapy cannot reliably distinguish tumour recurrence, atelectasis and RILT. A number of small studies have shown that DWI offers potential to troubleshoot in such cases, thus reducing the number of patients undergoing unnecessary invasive diagnostic procedures for benign lung change.[56,79] In addition to assessing response to treatment, DWI can potentially distinguish benign from malignant lymph nodes (benign having high ADC values)[80] and could play a role in radiotherapy-planning.[81]

New PET tracers

The need to evaluate more specific aspects of cancer biology other than glucose uptake has led to the development of new radiopharmaceuticals for potential future use in PET imaging.[82] ^{18}F-fluorothymidine (^{18}F-FLT) is a marker for cellular proliferation and correlates with the activity of thymidine kinase-1 (TK-1). It does not appear to accumulate in inflammatory cells, thereby offering improved specificity over ^{18}F-FDG PET/CT.[83] This tracer also has the potential to identify chemoradioresistant tumours post-treatment.[83] The response of tumours to treatment is influenced by the level of tumour oxygenation with intratumoral hypoxia increasing radio- and chemoresistance.[84] A number of tracers for imaging hypoxia have been developed. ^{18}F-FMISO, first used in cardiac imaging has been shown in clinical studies to have selectivity in NSCLC.[85] Angiogenesis (an important factor in the tumour microenvironment) can be assessed by targeted integrin PET imaging using ^{18}F-Galacto-RGD.[86] Although not currently

in clinical use, new PET tracers offer potential for planning individualised therapeutic regimens.

Artificial intelligence (AI), radiomics & deep-learning

CT, MRI and ^{18}F-FDG PET/CT are moving from primarily diagnostic tools for lung cancer towards having utility in prognostication and personalised medicine with the agency of AI.[87] Radiomics represents a non-invasive biomarker that draws on a subset of AI—Machine Learning (ML) to classify quantitative features associated with a given clinical end point.[88] The radiomics workflow involves manual segmentation of a region of interest (ROI) on a scan, from which features are extracted and pre-processed prior to classification[89,90] (Figure 10). Deep-learning is a subset of ML that describes a group of more complex algorithms. When applied to medical imaging, these facilitate automated segmentation, feature-extraction and identification of complex patterns in image data.[91] These approaches have shown promise in lung cancer diagnosis,[88,92–96] including a state-of-the-art deep-learning system for LDCT screening for pulmonary nodules (AUC = 0.944) which demonstrated similar performance to radiologists.[97] Additionally, they demonstrate ability in prognostication and evaluating response to treatment,[98–100] including a model that can estimate treatment failure following stereotactic body radiotherapy and guide individualisation of radiotherapy dose.[101]

CONCLUSION

Much progress has been made in the diagnosis and treatment of lung cancer in the past 20 years. Undoubtedly imaging has played a central role in this progress with the routine use of CT and ^{18}F-FDG PET/CT in staging and response evaluation, the use of MRI and DWI for "problem solving", automated and semi-automated assessment of solitary pulmonary nodules and targeted lung screening of high-risk populations. As we move towards tailored precision medicine based upon individual tumour and patient characteristics, the role of imaging will become ever more vital to ensure continued progress.

ACKNOWLEDGEMENTS

The authors gratefully acknowledge NHS National Institute of Health Research (NIHR) funding to the Royal Marsden Hospital and Institute of Cancer Research (ICR) London Biomedical Research Centre (BRC). Sumeet Hindocha is funded by the UKRI CDT in AI for Healthcare http://ai4health.io (Grant No. P/S023283/1).

REFERENCES

1. Bray F, Ferlay J, Soerjomataram I, Siegel RL, Torre LA, Jemal A. Global cancer statistics 2018: GLOBOCAN estimates of incidence and mortality worldwide for 36 cancers in 185 countries. *CA Cancer J Clin* 2018; **68**: 394–424. https://doi.org/10.3322/caac.21492
2. Allemani C, Matsuda T, Di Carlo V, Harewood R, Matz M, Nikšić M, et al. Global surveillance of trends in cancer survival 2000-14 (CONCORD-3): analysis of individual records for 37 513 025 patients diagnosed with one of 18 cancers from 322 population-based registries in 71 countries. *Lancet* 2018; **391**: 1023–75. https://doi.org/10.1016/S0140-6736(17)33326-3
3. Travis WD, Brambilla E, Nicholson AG, Yatabe Y, Austin JHM, Beasley MB, et al. The 2015 world health organization classification of lung tumors: impact of genetic, clinical and radiologic advances since the 2004 classification. *J Thorac Oncol* 2015; **10**: 1243–60. https://doi.org/10.1097/JTO.0000000000000630
4. Kandathil A, Kay FU, Butt YM, Wachsmann JW, Subramaniam RM. Role of FDG PET/CT in the eighth edition of TNM staging of non-small cell lung cancer. *Radiographics* 2018; **38**: 2134–49. https://doi.org/10.1148/rg.2018180060
5. Folch E, Costa DB, Wright J, VanderLaan PA. Lung cancer diagnosis and staging in the minimally invasive age with increasing demands for tissue analysis. *Transl Lung Cancer Res* 2015; **4**: 392–403. https://doi.org/10.3978/j.issn.2218-6751.2015.08.02
6. De Ruysscher D, Faivre-Finn C, Nestle U, Hurkmans CW, Le Péchoux C, Price A, et al. European organisation for research and treatment of cancer recommendations for planning and delivery of high-dose, high-precision radiotherapy for lung cancer. *J Clin Oncol* 2010; **28**: 5301–10. https://doi.org/10.1200/JCO.2010.30.3271
7. Ikeda N. Updates on minimally invasive surgery in non-small cell lung cancer. *Curr Treat Options Oncol* 2019; **20**: 16: 1–8: . https://doi.org/10.1007/s11864-019-0614-9
8. Herbst RS, Morgensztern D, Boshoff C. The biology and management of non-small cell lung cancer. *Nature* 2018; **553**: 446–54. https://doi.org/10.1038/nature25183
9. Sharma B, Martin A, Stanway S, Johnston SRD, Constantinidou A. Imaging in oncology -- over a century of advances. *Nat Rev Clin Oncol* 2012; **9**: 728–37. https://doi.org/10.1038/nrclinonc.2012.195
10. Carter BW, Lichtenberger JP III, Benveniste MK, de Groot PM, Wu CC, Erasmus JJ, et al. Revisions to the TNM staging of lung cancer: rationale, significance, and clinical application. *RadioGraphics* 2018; **38**: 374–91. https://doi.org/10.1148/rg.2018170081
11. Rami-Porta R, Bolejack V, Giroux DJ, Chansky K, Crowley J, Asamura H, et al. The IASLC lung cancer staging project: the new database to inform the eighth edition of the TNM classification of lung cancer. *J Thorac Oncol* 2014; **9**: 1618–24. https://doi.org/10.1097/JTO.0000000000000334
12. Rami-Porta R, Call S, Dooms C, Obiols C, Sánchez M, Travis WD, et al. Lung cancer staging: a concise update. *Eur Respir J* 2018; **51**: 1–17. https://doi.org/10.1183/13993003.00190-2018
13. Travis WD, Asamura H, Bankier AA, Beasley MB, Detterbeck F, Flieder DB, et al. The IASLC lung cancer staging project: proposals for coding T categories for subsolid nodules and assessment of tumor size in part-solid tumors in the forthcoming eighth edition of the TNM classification of lung cancer. *J Thorac Oncol* 2016; **11**: 1204–23. https://doi.org/10.1016/j.jtho.2016.03.025
14. Greenspan BS. Role of PET/CT for precision medicine in lung cancer: perspective of the Society of nuclear medicine and molecular imaging. *Transl Lung Cancer Res* 2017; **6**: 617–20. https://doi.org/10.21037/tlcr.2017.09.01
15. Lambe G, Durand M, Buckley A, Nicholson S, McDermott R. Adenocarcinoma of the lung: from BAC to the future. *Insights Imaging* 2020; **11**: 1–10. https://doi.org/10.1186/s13244-020-00875-6

16. Gelberg J, Grondin S, Tremblay A. Mediastinal staging for lung cancer. *Can Respir J* 2014; **21**: 159–61. https://doi.org/10.1155/2014/890108
17. Ganeshalingam S, Koh DM. Nodal staging. *Cancer Imaging* 2009; **9**: 104–11. https://doi.org/10.1102/1470-7330.2009.0017
18. van Tinteren H, Hoekstra OS, Smit EF, van den Bergh JHAM, Schreurs AJM, Stallaert RALM, et al. Effectiveness of positron emission tomography in the preoperative assessment of patients with suspected non-small-cell lung cancer: the plus multicentre randomised trial. *Lancet* 2002; **359**: 1388–93. https://doi.org/10.1016/s0140-6736(02)08352-6
19. Schimmer C, Neukam K, Elert O. Staging of non-small cell lung cancer: clinical value of positron emission tomography and mediastinoscopy. *Interact Cardiovasc Thorac Surg* 2006; **5**: 418–23. https://doi.org/10.1510/icvts.2006.129478
20. Kubota K, Matsuno S, Morioka N, Adachi S, Koizumi M, Seto H, et al. Impact of FDG-PET findings on decisions regarding patient management strategies: a multicenter trial in patients with lung cancer and other types of cancer. *Ann Nucl Med* 2015; **29**: 431–41. https://doi.org/10.1007/s12149-015-0963-9
21. Wu Y, Li P, Zhang H, Shi Y, Wu H, Zhang J, et al. Diagnostic value of fluorine 18 fluorodeoxyglucose positron emission tomography/computed tomography for the detection of metastases in non-small-cell lung cancer patients. *Int J Cancer* 2013; **132**: E37–47. https://doi.org/10.1002/ijc.27779
22. Beer L, Jajodia A, Prosch H. Pearls and pitfalls in lung cancer staging. 2020; **2**: 20200019: 20200019: . https://doi.org/10.1259/bjro.20200019
23. Lv Y-L, Yuan D-M, Wang K, Miao X-H, Qian Q, Wei S-Z, et al. Diagnostic performance of integrated positron emission tomography/computed tomography for mediastinal lymph node staging in non-small cell lung cancer: a bivariate systematic review and meta-analysis. *J Thorac Oncol* 2011; **6**: 1350–58. https://doi.org/10.1097/JTO.0b013e31821d4384
24. Taira AV, Herfkens RJ, Gambhir SS, Quon A. Detection of bone metastases: assessment of integrated FDG PET/CT imaging. *Radiology* 2007; **243**: 204–11. https://doi.org/10.1148/radiol.2431052104
25. Schmidt-Hansen M, Baldwin DR, Hasler E, Zamora J, Abraira V, Roqué I Figuls M. PET-CT for assessing mediastinal lymph node involvement in patients with suspected resectable non-small cell lung cancer. *Cochrane Database Syst Rev* 2014; **2014**(11). https://doi.org/10.1002/14651858.CD009519.pub2
26. Divisi D, Barone M, Crisci R. Current role of standardized uptake valuemax-derived ratios in N2 fluorine-18 fluorodeoxyglucose positron-emission tomography non-small cell lung cancer. *J Thorac Dis* 2018; **10**: 503–7. https://doi.org/10.21037/jtd.2017.11.137
27. Schumann SO, Kocher G, Minervini F. Epidemiology, diagnosis and treatment of the malignant pleural mesothelioma, a narrative review of literature. *J Thorac Dis* 2021; **13**: 2510–23. https://doi.org/10.21037/jtd-20-2761
28. Robinson BM. Malignant pleural mesothelioma: an epidemiological perspective. *Ann Cardiothorac Surg* 2012; **1**: 491–96. https://doi.org/10.3978/j.issn.2225-319X.2012.11.04
29. Nickell LT Jr, Lichtenberger JP 3rd, Khorashadi L, Abbott GF, Carter BW. Multimodality imaging for characterization, classification, and staging of malignant pleural mesothelioma. *Radiographics* 2014; **34**: 1692–1706. https://doi.org/10.1148/rg.346130089
30. Berzenji L, Van Schil PE, Carp L. The eighth TNM classification for malignant pleural mesothelioma. *Transl Lung Cancer Res* 2018; **7**: 543–49. https://doi.org/10.21037/tlcr.2018.07.05
31. de Perrot M, Dong Z, Bradbury P, Patsios D, Keshavjee S, Leighl NB, et al. Impact of tumour thickness on survival after radical radiation and surgery in malignant pleural mesothelioma. *Eur Respir J* 2017; **49**: 1–7. https://doi.org/10.1183/13993003.01428-2016
32. Rusch VW, Giroux D, Kennedy C, Ruffini E, Cangir AK, Rice D, et al. Initial analysis of the International association for the study of lung cancer mesothelioma database. *J Thorac Oncol* 2012; **7**: 1631–39. https://doi.org/10.1097/JTO.0b013e31826915f1
33. Armato SG, Nowak AK. Revised modified response evaluation criteria in solid tumors for assessment of response in malignant pleural mesothelioma (version 1.1). *J Thorac Oncol* 2018; **13**: 1012–21. https://doi.org/10.1016/j.jtho.2018.04.034
34. Rusch VW, Chansky K, Kindler HL, Nowak AK, Pass HI, Rice DC, et al. The IASLC mesothelioma staging project: proposals for the M descriptors and for revision of the TNM stage groupings in the forthcoming (eighth) edition of the TNM classification for mesothelioma. *J Thorac Oncol* 2016; **11**: 2112–19. https://doi.org/10.1016/j.jtho.2016.09.124
35. Hallifax RJ, Haris M, Corcoran JP, Leyakathalikhan S, Brown E, Srikantharaja D, et al. Role of CT in assessing pleural malignancy prior to thoracoscopy. *Thorax* 2015; **70**: 192–93. https://doi.org/10.1136/thoraxjnl-2014-206054
36. Heelan RT, Rusch VW, Begg CB, Panicek DM, Caravelli JF, Eisen C. Staging of malignant pleural mesothelioma: comparison of CT and MR imaging. *AJR Am J Roentgenol* 1999; **172**: 1039–47. https://doi.org/10.2214/ajr.172.4.10587144
37. Kruse M, Sherry SJ, Paidpally V, Mercier G, Subramaniam RM. FDG PET/CT in the management of primary pleural tumors and pleural metastases. *AJR Am J Roentgenol* 2013; **201**: W215–26. https://doi.org/10.2214/AJR.13.10572
38. Callister MEJ, Baldwin DR, Akram AR, Barnard S, Cane P, Draffan J, et al. British thoracic Society guidelines for the investigation and management of pulmonary nodules. *Thorax* 2015; **70 Suppl 2**: ii1–54. https://doi.org/10.1136/thoraxjnl-2015-207168
39. National Lung Screening Trial Research Team, Aberle DR, Adams AM, Berg CD, Black WC, Clapp JD, et al. Reduced lung-cancer mortality with low-dose computed tomographic screening. *N Engl J Med* 2011; **365**: 395–409. https://doi.org/10.1056/NEJMoa1102873
40. MacMahon H, Naidich DP, Goo JM, Lee KS, Leung ANC, Mayo JR, et al. Guidelines for management of incidental pulmonary nodules detected on CT images: from the fleischner society 2017. *Radiology* 2017; **284**: 228–43. https://doi.org/10.1148/radiol.2017161659
41. Nair A, Devaraj A, Callister MEJ, Baldwin DR. The fleischner Society 2017 and British thoracic Society 2015 guidelines for managing pulmonary nodules: keep calm and carry on. *Thorax* 2018; **73**: 806–12. https://doi.org/10.1136/thoraxjnl-2018-211764
42. McWilliams A, Tammemagi MC, Mayo JR, Roberts H, Liu G, Soghrati K, et al. Probability of cancer in pulmonary nodules detected on first screening CT. *N Engl J Med* 2013; **369**: 910–19. https://doi.org/10.1056/NEJMoa1214726
43. Herder GJ, van Tinteren H, Golding RP, Kostense PJ, Comans EF, Smit EF, et al. Clinical prediction model to characterize pulmonary nodules: validation and added value of 18F-fluorodeoxyglucose positron emission tomography. *Chest* 2005; **128**: 2490–96. https://doi.org/10.1378/chest.128.4.2490
44. Al-Ameri A, Malhotra P, Thygesen H, Plant PK, Vaidyanathan S, Karthik S, et al. Risk of malignancy in pulmonary nodules: a validation study of four prediction models. *Lung Cancer* 2015; **89**: 27–30. https://doi.org/10.1016/j.lungcan.2015.03.018

45. Nagata Y, Matsuo Y, Takayama K, Norihisa Y, Mizowaki T, Mitsumori M, et al. Current status of stereotactic body radiotherapy for lung cancer. *Int J Clin Oncol* 2007; **12**: 3–7. https://doi.org/10.1007/s10147-006-0646-6
46. Haidar YM, Rahn DA 3rd, Nath S, Song W, Bazhenova L, Makani S, et al. Comparison of outcomes following stereotactic body radiotherapy for non-small cell lung cancer in patients with and without pathological confirmation. *Ther Adv Respir Dis* 2014; **8**: 3–12. https://doi.org/10.1177/1753465813512545
47. Louie AV, Senan S, Patel P, Ferket BS, Lagerwaard FJ, Rodrigues GB, et al. When is a biopsy-proven diagnosis necessary before stereotactic ablative radiotherapy for lung cancer?: a decision analysis. *Chest* 2014; **146**: 1021–28. https://doi.org/10.1378/chest.13-2924
48. Sebastian NT, Xu-Welliver M, Williams TM. Stereotactic body radiation therapy (SBRT) for early stage non-small cell lung cancer (NSCLC): contemporary insights and advances. *J Thorac Dis* 2018; **10**: S2451–64. https://doi.org/10.21037/jtd.2018.04.52
49. Dyer SC, Bartholmai BJ, Koo CW. Implications of the updated lung CT screening reporting and data system (lung-RADS version 1.1) for lung cancer screening. *J Thorac Dis* 2020; **12**: 6966–77. https://doi.org/10.21037/jtd-2019-cptn-02
50. Oudkerk M, Devaraj A, Vliegenthart R, Henzler T, Prosch H, Heussel CP, et al. European position statement on lung cancer screening. *Lancet Oncol* 2017; **18**: e754–66. https://doi.org/10.1016/S1470-2045(17)30861-6
51. Martin MD, Kanne JP, Broderick LS, Kazerooni EA, Meyer CA. Lung-RADS: pushing the limits. *Radiographics* 2017; **37**: 1975–93. https://doi.org/10.1148/rg.2017170051
52. Pinsky PF, Gierada DS, Black W, Munden R, Nath H, Aberle D, et al. Performance of lung-RADS in the National lung screening trial: a retrospective assessment. *Ann Intern Med* 2015; **162**: 485–91. https://doi.org/10.7326/M14-2086
53. McKee BJ, Regis SM, McKee AB, Flacke S, Wald C. Performance of ACR lung-RADS in a clinical CT lung screening program. *J Am Coll Radiol* 2016; **13**: R25–9. https://doi.org/10.1016/j.jacr.2015.12.009
54. Kastner J, Hossain R, Jeudy J, Dako F, Mehta V, Dalal S, et al. Lung-RADS version 1.0 versus lung-RADS version 1.1: comparison of categories using nodules from the National lung screening trial. *Radiology* 2021; **300**: 199–206. https://doi.org/10.1148/radiol.2021203704
55. Mayo JR, Lam S. Doing too much or not enough: striking a balance. *Radiology* 2021; **300**: 207–8. https://doi.org/10.1148/radiol.2021210774
56. Jagoda P, Fleckenstein J, Sonnhoff M, Schneider G, Ruebe C, Buecker A, et al. Diffusion-weighted MRI improves response assessment after definitive radiotherapy in patients with NSCLC. *Cancer Imaging* 2021; **21**: 15. https://doi.org/10.1186/s40644-021-00384-9
57. Eisenhauer EA, Therasse P, Bogaerts J, Schwartz LH, Sargent D, Ford R, et al. New response evaluation criteria in solid tumours: revised RECIST guideline (version 1.1). *Eur J Cancer* 2009; **45**: 228–47. https://doi.org/10.1016/j.ejca.2008.10.026
58. Coche E. Evaluation of lung tumor response to therapy: current and emerging techniques. *Diagn Interv Imaging* 2016; **97**: 1053–65. https://doi.org/10.1016/j.diii.2016.09.001
59. Dunlap NE, Yang W, McIntosh A, Sheng K, Benedict SH, Read PW, et al. Computed tomography-based anatomic assessment overestimates local tumor recurrence in patients with mass-like consolidation after stereotactic body radiotherapy for early-stage non-small cell lung cancer. *Int J Radiat Oncol Biol Phys* 2012; **84**: 1071–77. https://doi.org/10.1016/j.ijrobp.2012.01.088
60. Byrne MJ, Nowak AK. Modified RECIST criteria for assessment of response in malignant pleural mesothelioma. *Ann Oncol* 2004; **15**: 257–60. https://doi.org/10.1093/annonc/mdh059
61. Anderson O, Kidd AC, Goatman K, Weir A, Voisey J, Dilys V, et al. Estimating the false positive prediction rate in automated volumetric measurements of malignant pleural mesothelioma. *Communication in Computer and Information Science* 2021; 116–39.
62. Mozley PD, Bendtsen C, Zhao B, Schwartz LH, Thorn M, Rong Y, et al. Measurement of tumor volumes improves RECIST-based response assessments in advanced lung cancer. *Translational Oncology* 2012; **5**: 19–25. https://doi.org/10.1593/tlo.11232
63. Ganeshan B, Panayiotou E, Burnand K, Dizdarevic S, Miles K. Tumour heterogeneity in non-small cell lung carcinoma assessed by CT texture analysis: a potential marker of survival. *Eur Radiol* 2012; **22**: 796–802. https://doi.org/10.1007/s00330-011-2319-8
64. Ravanelli M, Farina D, Morassi M, Roca E, Cavalleri G, Tassi G, et al. Texture analysis of advanced non-small cell lung cancer (NSCLC) on contrast-enhanced computed tomography: prediction of the response to the first-line chemotherapy. *Eur Radiol* 2013; **23**: 3450–55. https://doi.org/10.1007/s00330-013-2965-0
65. Yabuuchi H, Kawanami S, Iwama E, Okamoto I, Kamitani T, Sagiyama K, et al. Prediction of therapeutic effect of chemotherapy for NSCLC using dual-input perfusion CT analysis: comparison among bevacizumab treatment, two-agent platinum-based therapy without bevacizumab, and other non-bevacizumab treatment groups. *Radiology* 2018; **286**: 685–95. https://doi.org/10.1148/radiol.2017162204
66. Otrakji A, Digumarthy SR, Lo Gullo R, Flores EJ, Shepard J-AO, Kalra MK. Dual-Energy CT: spectrum of thoracic abnormalities. *RadioGraphics* 2016; **36**: 38–52. https://doi.org/10.1148/rg.2016150081
67. Kandathil A, Carson R, Subramaniam R. Lung cancer recurrence: 18 F-FDG PET/CT in clinical practice. *Nuc Med Mol Imag* 2019; 1136–2019.
68. Wahl RL, Jacene H, Kasamon Y, Lodge MA. From RECIST to PERCIST: evolving considerations for PET response criteria in solid tumors. *J Nucl Med* 2009; **50 Suppl 1**: 122S–50S. https://doi.org/10.2967/jnumed.108.057307
69. O JH, Lodge MA, Wahl RL. Practical PERCIST: a simplified guide to PET response criteria in solid tumors 1.0. *Radiology* 2016; **280**: 576–84. https://doi.org/10.1148/radiol.2016142043
70. Shang J, Ling X, Zhang L, Tang Y, Xiao Z, Cheng Y, et al. Comparison of recist, EORTC criteria and PERCIST for evaluation of early response to chemotherapy in patients with non-small-cell lung cancer. *Eur J Nucl Med Mol Imaging* 2016; **43**: 1945–53. https://doi.org/10.1007/s00259-016-3420-7
71. Jiang X, Dudzinski S, Beckermann KE, Young K, McKinley E, J McIntyre O, et al. MRI of tumor T cell infiltration in response to checkpoint inhibitor therapy. *J Immunother Cancer* 2020; **8**: 1–12. https://doi.org/10.1136/jitc-2019-000328
72. Borcoman E, Nandikolla A, Long G, Goel S, Le Tourneau C. Patterns of response and progression to immunotherapy. *American Society of Clinical Oncology Educational Book* 2018; :: 169–78. https://doi.org/10.1200/EDBK_200643
73. Seymour L, Bogaerts J, Perrone A, Ford R, Schwartz LH, Mandrekar S, et al. IRECIST: guidelines for response criteria for use in trials testing immunotherapeutics. *Lancet Oncol* 2017; **18**: e143–52. https://doi.org/10.1016/S1470-2045(17)30074-8
74. Champiat S, Dercle L, Ammari S, Massard C, Hollebecque A, Postel-Vinay S, et al.

Hyperprogressive disease is a new pattern of progression in cancer patients treated by anti-PD-1/PD-L1. *Clin Cancer Res* 2017; **23**: 1920–28. https://doi.org/10.1158/1078-0432.CCR-16-1741
75. Kato S, Goodman A, Walavalkar V, Barkauskas DA, Sharabi A, Kurzrock R. Hyperprogressors after immunotherapy: analysis of genomic alterations associated with accelerated growth rate. *Clin Cancer Res* 2017; **23**: 4242–50. https://doi.org/10.1158/1078-0432.CCR-16-3133
76. Taylor SA, Mallett S, Ball S, Beare S, Bhatnagar G, Bhowmik A, et al. Diagnostic accuracy of whole-body MRI versus standard imaging pathways for metastatic disease in newly diagnosed non-small-cell lung cancer: the prospective streamline L trial. *The Lancet Respiratory Medicine* 2019; **7**: 523–32. https://doi.org/10.1016/S2213-2600(19)30090-6
77. Navani N, Nankivell M, Lawrence DR, Lock S, Makker H, Baldwin DR, et al. Lung cancer diagnosis and staging with endobronchial ultrasound-guided transbronchial needle aspiration compared with conventional approaches: an open-label, pragmatic, randomised controlled trial. *Lancet Respir Med* 2015; **3**: 282–89. https://doi.org/10.1016/S2213-2600(15)00029-6
78. Regier M, Derlin T, Schwarz D, Laqmani A, Henes FO, Groth M, et al. Diffusion weighted MRI and 18F-FDG PET/CT in non-small cell lung cancer (NSCLC): does the apparent diffusion coefficient (ADC) correlate with tracer uptake (SUV)? *Eur J Radiol* 2012; **81**: 2913–18. https://doi.org/10.1016/j.ejrad.2011.11.050
79. Munoz-Schuffenegger P, Kandel S, Alibhai Z, Hope A, Bezjak A, Sun A, et al. A prospective study of magnetic resonance imaging assessment of post-radiation changes following stereotactic body radiation therapy for non-small cell lung cancer. *Clin Oncol (R Coll Radiol)* 2019; **31**: 720–27. https://doi.org/10.1016/j.clon.2019.05.014
80. Shen G, Hu S, Deng H, Kuang A. Performance of DWI in the nodal characterization and assessment of lung cancer: a meta-analysis. *AJR Am J Roentgenol* 2016; **206**: 283–90. https://doi.org/10.2214/AJR.15.15032
81. Fleckenstein J, Jelden M, Kremp S, Jagoda P, Stroeder J, Khreish F, et al. The impact of diffusion-weighted MRI on the definition of gross tumor volume in radiotherapy of non-small-cell lung cancer. *PLoS ONE* 2016; **11**: e0162816. https://doi.org/10.1371/journal.pone.0162816
82. Theodoropoulos AS, Gkiozos I, Kontopyrgias G, Charpidou A, Kotteas E, Kyrgias G, et al. Modern radiopharmaceuticals for lung cancer imaging with positron emission tomography/computed tomography scan: a systematic review. *SAGE Open Medicine* 2020; **8**: 205031212096159. https://doi.org/10.1177/2050312120961594
83. Bollineni VR, Kramer GM, Jansma EP, Liu Y, Oyen WJG. A systematic review on [(18)F]FLT-PET uptake as A measure of treatment response in cancer patients. *Eur J Cancer* 2016; **55**: 81–97. https://doi.org/10.1016/j.ejca.2015.11.018
84. Vaupel P, Mayer A. Hypoxia in cancer: significance and impact on clinical outcome. *Cancer Metastasis Rev* 2007; **26**: 225–39. https://doi.org/10.1007/s10555-007-9055-1
85. Vera P, Bohn P, Edet-Sanson A, Salles A, Hapdey S, Gardin I. Simultaneous positron emission tomography (PET) assessment of metabolism with 18F-fluoro-2-deoxy-d-glucose (FDG), proliferation with 18F-fluoro-thymidine (FLT), and hypoxia with 18fluoro-misonidazole (F-miso) before and during radiotherapy in patients with non-small-cell lung cancer (NSCLC): A pilot study. *Radiother Oncol* 2011; **98**: 109–16. https://doi.org/10.1016/j.radonc.2010.10.011
86. Li L, Zhao W, Sun X, Liu N, Zhou Y, Luan X, et al. 18f-RGD PET/CT imaging reveals characteristics of angiogenesis in non-small cell lung cancer. *Transl Lung Cancer Res* 2020; **9**: 1324–32. https://doi.org/10.21037/tlcr-20-187
87. Hunter B, Hindocha S, Lee RW. The role of artificial intelligence in early cancer diagnosis. *Cancers (Basel)* 2022; **14**(6): 1524. https://doi.org/10.3390/cancers14061524
88. Aerts HJWL, Velazquez ER, Leijenaar RTH, Parmar C, Grossmann P, Carvalho S, et al. Correction: corrigendum: decoding tumour phenotype by noninvasive imaging using a quantitative radiomics approach. *Nat Commun* 2014; **5**: 1–8. https://doi.org/10.1038/ncomms5644
89. Lambin P, Leijenaar RTH, Deist TM, Peerlings J, de Jong EEC, van Timmeren J, et al. Radiomics: the bridge between medical imaging and personalized medicine. *Nat Rev Clin Oncol* 2017; **14**: 749–62. https://doi.org/10.1038/nrclinonc.2017.141
90. van Timmeren JE, Cester D, Tanadini-Lang S, Alkadhi H, Baessler B. Radiomics in medical imaging-"how-to" guide and critical reflection. *Insights Imaging* 2020; **11**: 91. https://doi.org/10.1186/s13244-020-00887-2
91. Hosny A, Aerts HJ, Mak RH. Handcrafted versus deep learning radiomics for prediction of cancer therapy response. *Lancet Digit Health* 2019; **1**: e106–7. https://doi.org/10.1016/S2589-7500(19)30062-7
92. Wu G, Woodruff HC, Shen J, Refaee T, Sanduleanu S, Ibrahim A, et al. Diagnosis of invasive lung adenocarcinoma based on chest CT radiomic features of part-solid pulmonary nodules: a multicenter study. *Radiology* 2020; **297**: 451–58. https://doi.org/10.1148/radiol.2020192431
93. Nishio M, Sugiyama O, Yakami M, Ueno S, Kubo T, Kuroda T, et al. Computer-Aided diagnosis of lung nodule classification between benign nodule, primary lung cancer, and metastatic lung cancer at different image size using deep convolutional neural network with transfer learning. *PLoS One* 2018; **13**(7): e0200721. https://doi.org/10.1371/journal.pone.0200721
94. Binczyk F, Prazuch W, Bozek P, Polanska J. Radiomics and artificial intelligence in lung cancer screening. *Transl Lung Cancer Res* 2021; **10**: 1186–99. https://doi.org/10.21037/tlcr-20-708
95. Ciompi F, Chung K, van Riel SJ, Setio AAA, Gerke PK, Jacobs C, et al. Towards automatic pulmonary nodule management in lung cancer screening with deep learning. *Sci Rep* 2017; **7**: 46479. https://doi.org/10.1038/srep46479
96. Avanzo M, Stancanello J, Pirrone G, Sartor G. Radiomics and deep learning in lung cancer. *Strahlenther Onkol* 2020; **196**: 879–87. https://doi.org/10.1007/s00066-020-01625-9
97. Ardila D, Kiraly AP, Bharadwaj S, Choi B, Reicher JJ, Peng L, et al. End-To-End lung cancer screening with three-dimensional deep learning on low-dose chest computed tomography. *Nat Med* 2019; **25**: 954–61. https://doi.org/10.1038/s41591-019-0447-x
98. Xu Y, Hosny A, Zeleznik R, Parmar C, Coroller T, Franco I, et al. Deep learning predicts lung cancer treatment response from serial medical imaging. *Clin Cancer Res* 2019; **25**: 3266–75. https://doi.org/10.1158/1078-0432.CCR-18-2495
99. Baek S, He Y, Allen BG, Buatti JM, Smith BJ, Tong L, et al. Deep segmentation networks predict survival of non-small cell lung cancer. *Sci Rep* 2019; **9**: 17286. https://doi.org/10.1038/s41598-019-53461-2
100. Chetan MR, Gleeson FV. Radiomics in predicting treatment response in non-small-cell lung cancer: current status, challenges and future perspectives. *Eur Radiol* 2021; **31**: 1049–58. https://doi.org/10.1007/s00330-020-07141-9
101. Lou B, Doken S, Zhuang T, Wingerter D, Gidwani M, Mistry N, et al. An image-based deep learning framework for individualising radiotherapy dose: a retrospective analysis of outcome prediction. *The Lancet Digital Health* 2019; **1**: e136–47. https://doi.org/10.1016/S2589-7500(19)30058-5